Biomedicine & Pharmacotherapy 165 (2023) 115235

Contents lists available at ScienceDirect

Biomedicine & Pharmacotherapy

journal homepage: www.elsevier.com/locate/biopha

Uncovering the expression of circPVT1 in the extracellular vesicles of acute myeloid leukemia patients

Martina Ghetti [a,1], Ivan Vannini [b,1], Maria Teresa Bochicchio [a], Irene Azzali [c], Lorenzo Ledda [a], Giovanni Marconi [d], Mattia Melloni [e], Francesco Fabbri [a], Michela Rondoni [f], Roberta Chicchi [g], Davide Angeli [c], Andrea Ghelli Luserna di Rorà [a,h], Barbara Giannini [i], Irene Zacheo [d], Rino Biguzzi [g], Francesco Lanza [f], Giovanni Martinelli [j], Giorgia Simonetti [a,*]

[a] Biosciences Laboratory, IRCCS Istituto Romagnolo per lo Studio dei Tumori (IRST) "Dino Amadori", Meldola, Italy
[b] Pathology Unit, Morgagni-Pierantoni Hospital, AUSL Romagna, Forlì, Italy
[c] Unit of Biostatistics and Clinical Trials, IRCCS Istituto Romagnolo per lo Studio dei Tumori (IRST) "Dino Amadori", Meldola, Italy
[d] Hematology Unit, IRCCS Istituto Romagnolo per lo Studio dei Tumori (IRST) "Dino Amadori", Meldola, Italy
[e] Laboratory of Biomarkers, Biomolecular Targets and Personalized Medicine in Oncology, Translational Medicine, University of Ferrara, Ferrara, Italy
[f] Hematology Unit & Romagna Transplant Network, Ravenna Hospital, Ravenna, Italy
[g] Laboratorio Unico AUSL della Romagna, U.O. Medicina Trasfusionale di Forlì-Cesena e Officina Trasfusionale della Romagna, Pievesestina di Cesena, Italy
[h] Fondazione Pisana per la Scienza ONLUS, San Giuliano Terme, Italy
[i] Laboratorio Unico AUSL della Romagna, U.O. Genetica Medica, Pievesestina di Cesena, Italy
[j] Scientific Directorate, IRCCS Istituto Romagnolo per lo Studio dei Tumori (IRST) "Dino Amadori", Meldola, Italy

ARTICLE INFO

Keywords:
CirRNA
CircPVT1
Acute myeloid leukemia
Extracellular vesicles
Immune system

ABSTRACT

Extracellular vesicles (EVs) act as molecular mediators in the tumor microenvironment, by shuttling information contained within malignant cells and functioning as regulators of the immune system. Circular (circ)RNAs are characterized by a closed loop-like structure that makes them more stable in the extracellular milieu and suitable to be packaged inside EVs. circPVT1 (hsa_circ_0001821) showed an oncogenic role in several cancer types and immunosuppressive properties in myeloid and lymphoid cell subsets. In this study, we characterized EVs from acute myeloid leukemia (AML) patients in terms of size, concentrations, surface markers and circPVT1 cargo. We showed that circPVT1 is overexpressed by primary blast cells from newly-diagnosed AML patients compared with hematopoietic stem-progenitor cells and is released as cell-free RNA in the plasma. We isolated EVs from the plasma of AML patients and healthy subjects by size exclusion chromatography and characterized them by nanoparticle tracking analysis. EVs from patients' plasma are larger compared with those from healthy subjects and their surface profile is characterized by higher levels of the leukemic cell markers CD133, CD105, CD49e and other immune-related epitopes, with differences according to AML molecular profile. Moreover, digital PCR analysis revealed that circPVT1 is more abundant inside EVs from the plasma of AML patients compared with healthy subjects. Our findings provide new insights on the features and content of AML EVs and suggest a role of circPVT1 in the crosstalk between AML cells and the tumor microenvironment.

1. Introduction

Extracellular vesicles (EVs) are recognized as a new class of molecular mediators in the tumor microenvironment. EVs transfer the information contained within malignant cells into the tumor microenvironment, thus regulating many cellular processes. In acute myeloid leukemia (AML), EVs were reported to suppress normal hematopoiesis and to protect blast cells from chemotherapeutic agents [1–4]. Moreover, AML EVs can suppress immune response, specifically through the release of cargo molecules that interferes with NK cells and their NKG2D receptor or through induction of apoptosis in human activated T cells [5–7].

* Correspondence to: Biosciences Laboratory, IRCCS Istituto Romagnolo per lo Studio dei Tumori (IRST) "Dino Amadori", via Piero Maroncelli 40, 47014 Meldola, FC, Italy.
E-mail address: giorgia.simonetti@irst.emr.it (G. Simonetti).
[1] These authors contributed equally to the work.

https://doi.org/10.1016/j.biopha.2023.115235
Received 18 May 2023; Received in revised form 19 July 2023; Accepted 25 July 2023
Available online 1 August 2023

EVs contain protein, DNA, mRNA, short and long non-coding RNAs (ncRNAs), which include circular (circ)RNAs. The latter are characterized by a covalently closed loop-like structure with no 5′ and 3′ polarity conferring a remarkable stability [8].

Evidence suggests an oncogenic role of circRNAs in AML [9]. They are involved in the regulation of cell cycle and leukemic cell proliferation, apoptosis and chemo-sensitivity through miRNA sponging. This activity is mediated by circRNAs alterations both at intracellular and exosome level [10,11]. Indeed, circ_0009910 shuttled by EVs, favors proliferation and cell cycle progression, while inhibiting apoptosis of AML cells partially through regulation of the miR-5195–3p/GRB10 axis [12]. In addition, exosome-mediated circ_0004136 knockdown hampered the acquisition of an aggressive AML phenotype by acting on the miR-570–3p/TSPAN3 axis [13].

circPVT1 (hsa_circ_0001821) is encoded by the human Plasmacytoma Variant Translocation 1 (*PVT1*) gene, which is located on chromosome band 8q24.21 [14]. The gene encodes for 190 linear isoforms (www.ensembl.org/index.html) and 26 circular isoforms (circinteractome.nia.nih.gov and www.circbase.org). Hsa_circ_0001821 is the most common circular *PVT1* isoform, a 410 bp product of back-splicing, and contains the entire exon 2 of *PVT1* in a closed loop-like structure. circPVT1 has pro-tumorigenic functions when overexpressed in several cancer types [15] and has a potential prognostic value in AML [16]. Recently, a novel fascinating role has been suggested in the regulation of immune responses [14]. Specifically, circPVT1 was significantly reduced in monocytes, B and T lymphocytes from the peripheral blood (PB) of patients affected by Systemic Lupus Erythematosus and the low levels contributed to the aberrant activation of the interferon (IFN)-inducible serine/threonine protein kinase PKR, which plays a role in innate immunity [17]. We can therefore hypothesize that circPVT1 may function as extracellular entity in the crosstalk between leukemia and the tumor microenvironment.

In this study we characterized the EVs isolated from the peripheral blood of newly-diagnosed AML patients in terms of size and surface protein expression, and compared them with EVs collected from healthy subjects. Moreover, we analyzed the extracellular levels of circPVT1 (hsa_circ_0001821) within EVs isolated from AML patients.

2. Materials and methods

2.1. Sample collection and cell preparation

Samples were obtained from newly-diagnosed adult AML patients and healthy subjects after written informed consent, as approved by the Institutional Ethics Committees (Comitato Etico Indipendente di Area Vasta Emilia Centro, protocol 112/2014/U/Tess and Comitato Etico della Romagna, protocol 5805/2019), in accordance with the Declaration of Helsinki. Mononuclear cells from bone marrow (BMMCs, n = 11) of AML (non acute promyelocytic leukemia) were collected by density gradient centrifugation using Lymphosep (Biowest). Healthy stem-progenitor cells ($CD34^+$) from bone marrow specimens (n = 7) were obtained from STEMCELL Technologies Inc.

2.2. Plasma samples collection

EDTA blood samples were collected from AML patients (n = 18) and healthy subjects (n = 12). Platelet-free plasma samples were prepared within 2 h after collection, by centrifugation at 2500 g for 15 min at room temperature. Aliquots were stored at − 80 °C until use.

2.3. DNA extraction and molecular profiling

DNA was extracted from primary mononuclear cells (BMMCs or PBMCs, n = 18) using the Maxwell® RSC Blood DNA Kit (Promega Corporation) according to the manufacturer's instructions. The mutational profile of patients was determined using the Myeloid Solution panel (SOPHiA GENETICS). Libraries were prepared according to the manufacturer's recommendations and quantified using the Qubit® dsDNA High Sensitivity Assay on a Qubit® Fluorometer (Thermo Fisher Scientific, Inc.). Amplicons were determined by capillary electrophoresis using Agilent High Sensitivity DNA kit (Agilent Technologies, Inc.). The pooled libraries were paired-end (2 ×301) and sequenced with v3 chemistry on a MiSeq™ instrument (Illumina, Inc.), as described in the manufacturer's protocol. FASTQ sequencing files were analyzed by SOPHiA DDM™ platform (Pipeline ILL1XG1S9_CNV_1). The Human Genome Build 19 (Hg19) was used as the reference for sequence alignment. The minimum coverage depth was set at 1,000x; single-nucleotide polymorphisms, variants localized in intronic and UTR regions and synonymous variants were excluded. Only exonic and splice site variants with a variant allele frequency (VAF) ≥ 2.5% were evaluated. The variants were annotated according to the ACMG rules using Varsome, and benign and likely benign variants were discarded. Oncoprint was obtained with ComplexHeatmap R Package [18].

2.4. EVs isolation and NanoSight Tracking Analysis (NTA)

EVs enriched fractions were isolated from plasma samples by size-exclusion chromatography (SEC) columns of polysaccharide resin (qEV 70 columns; IZON), according to manufacturer's protocol. The size and concentration of isolated EVs were evaluated by NanoSight NS300 instrument (Malvern Instruments), equipped with NTA 2.3 analytical software laser. Briefly, samples diluted in 0.1 μm filtered PBS were analyzed. Three videos of 30 s each per sample were obtained with a camera level of 15 and in light scattering mode as indicated in the manufacturer's protocol.

2.5. EV surface protein analysis

EV surface proteins (n = 37 epitopes) were analyzed through a Bead-based multiplex EV analysis by flow cytometry (MACSPlex Exosome Kit, human; Miltenyi Biotec). EVs were processed as follows: the MACSPlex buffer (MPB) was added to EVs SEC eluate, then different antibody-coated bead subsets and APC-conjugated anti-CD9, anti-CD63, and anti-CD81 detection antibodies were added to each sample and incubated for 1 h at room temperature on an orbital shaker. MPB washes were performed on samples following the company's protocol. The median fluorescence intensity (MFI) for each epitope was obtained by flow cytometry analysis (BD FACSCanto, BD Biosciences). The MFI value of each epitope was corrected by subtracting the MFI value of blank control.

2.6. RNA extraction

RNA was extracted from EVs using the Plasma/Serum RNA Purification Mini Kit (Norgen, Biotek Corporation) following the manufacturer's instructions. Specifically, starting from 200 μL of EVs enriched fractions, the purified RNA is eluted in a volume of 20 μL. Cell-free RNA was isolated from plasma samples using TRIzol™ LS Reagent (Invitrogen™), starting from 250 μL plasma samples and a final resuspension of the pellet obtained of 20 μL in RNAse free water. RNA was obtained from cells by TRIzol™ extraction, according to manufacturer's recommendations and with a final resuspension in RNAse free water of 30 μL. Total RNA yield was assessed by NanoDrop.

2.7. Quantitative reverse-transcription polymerase chase reaction (qRT-PCR)

RNA from cells was reverse transcribed into cDNA using the PrimeScript Reag Kit with gDNA Eraser (Takara Bio Inc). RNA from EVs and cell-free RNA was reverse transcribed into cDNA using SuperScript™ VILO™ cDNA Synthesis Kit (Invitrogen™). TaqMan gene expression analysis of *PVT1* (Hs01069025_m1, ThermoFisher Scientific Inc.) and

circPVT1 (custom assay, ThermoFisher Scientific Inc.) and of HPRT1 (Hs02800695_m1, ThermoFisher Scientific Inc.) as reference gene was performed on the Applied Biosystems 7500 Real-Time PCR System (ThermoFisher Scientific Inc.). Gene expression was quantified by the $2^{-\Delta Ct}$ or $2^{-\Delta\Delta Ct}$ methods.

2.8. Digital (d)PCR

dPCR experiments were carried out using the chip-based QuantStudioTM 3D Digital PCR system (Thermo Fisher Scientific Inc.). Reaction mix containing either 6 μL cDNA or water (no-template controls) were prepared by adding 8.5 μL 2X QuantStudio 3D™ Digital PCR Master Mix v2 (Thermo Fisher Scientific Inc.) and 1 μL 20X gene circPVT1 (custom Taqman assay, Thermo Fisher Scientific Inc.) assay in a total volume of 15.5 μL. Chips were run on the GeneAmp PCR System 9700 (Thermo Fisher Scientific Inc.) by applying the following conditions: hold at 96 °C for 10 min; 45 cycles of 60 °C for 2 min and 98 °C for 30 s; hold at 60 °C for 2 min. Chips were then processed using the QuantStudio™ 3D Digital PCR system (Thermo Fisher Scientific Inc.) and analyzed by QuantStudio™ 3D Analysis Suite™ software (version 3.0.3) [19]. circPVT1 relative quantification was obtained by normalization of its expression level (copies/μL) on the number of EVs.

2.9. Statistical analyses

Data were reported as mean and standard deviation or median and interquartile range for continuous variables and by frequencies and percentages for categorical ones. The Mann-Whitney U test was used to compare continuous values over categories. Correlation between continuous variables was measured by Spearman's correlation coefficient. All *p*-values were obtained by a two-sided testing and were valued significant when their value was ≤ 0.05. Due to the exploratory nature of the study no p-value correction for multiple comparison was performed. Statistical analyses were carried out using R software v4.2.2.

3. Results

3.1. circPVT1 expression in leukemic cells and in cell-free RNA from AML patients

Our cohort consisted of 18 newly-diagnosed AML patients that were assessed for cytogenetics and mutational profile. Thirteen of them were classified as adverse-risk (72.2%), 3 as intermediate-risk (16.7%) and 2 as favorable risk (11.1%), according to European Leukemia Net (ELN) 2022 (Table 1). BMMCs were available from 11 samples (9 adverse risk, 1 intermediate risk and 1 favorable risk). In those cases, we analyzed the level of circPVT1 expression compared with $CD34^+$ BM cells from healthy subjects (n = 7). circPVT1 was overexpressed in AML cells compared with normal $CD34^+$ cells ($p = 0.006$, Fig. 1A). No significant differences were observed in the AML cohort when stratifying patients according to the risk categories or mutations (Fig. 1B and Table S1). Since the circular structure confers circRNAs a high level of stability and resistance to the exonuclease activity of RNase R, we asked whether circPVT1 was released in the patients' plasma [8,20]. circPVT1 was detectable as cell-free RNA in the plasma of AML patients and at higher levels compared with linear *PVT1* (Fig. 1C), suggesting that circPVT1 can serve as a preferred mediator in the crosstalk between leukemia cells and the microenvironment compared with the linear isoforms. When comparing cell-free circPVT1 levels between AML and healthy subjects, we observed higher circRNA expression in the latter ($p = 0.022$, Fig. 1D).

3.2. Characterization of size and number of EVs in the plasma of AML patients compared with healthy subjects

Since circRNAs can be encapsulated within EVs, we decided to first characterize circulating EVs isolated from the plasma of AML patients (n = 18, Table 1) in comparison with EVs isolated from healthy subjects (n = 12). EVs were isolated by SEC and characterized by NTA in terms of size and concentration. Representative NTA profiles are reported in Fig. 2A.

EV total concentrations were not different between the two cohorts. When dividing EVs by size, we observed that the relative concentration of EVs with a diameter between 50 nm and 150 nm was higher in healthy subjects compared with AML patients (AML median concentration 0.67, range 0.34–0.89, *versus* healthy median concentration 0.82, range 0.67–0.87; $p = 0.047$, Fig. 2B). Conversely, EVs with a diameter between 150 and 300 nm showed a higher concentration in AML patients compared with healthy subjects (AML median concentration 0.31, range 0.08–0.54 *versus* healthy median concentration 0.17, range 0.11–0.31; $p = 0.04$, Fig. 2C). When analyzing the average EV size, we observed that the average EV diameter was higher in AML patients compared with healthy subjects (median of AML EV diameter, 135.83 nm, range 85.27–174.72 *versus* median of healthy EV diameter, 111.86 nm, range 103.60–132.63; $p = 0.04$, Fig. 2D). Association studies between the patients' mutational profile and EV total concentrations suggested lower levels of EVs in the plasma of *SRSF2*-mutated (mut, n = 5 *versus* wildtype, n = 10, $p = 0.02$, Fig. 2E) AML compared with wildtype cases. Moreover, we observed differences according to ELN 2022 classification ($p = 0.01$, Fig. 2F), with intermediate and high risk patients showing high and low EV concentration, respectively.

Table 1
Patient's characteristics and analyses.

Pt ID	Sex	Age	ELN 2022 classification	EVs Number	Intracellular circPVT1	cell-free circPVT1	EVs circPVT1
1	F	66	Adverse	1.14×10^{11}	5.247	0.585	2.25×10^{-12}
2	F	54	Intermediate	2.38×10^{11}	NA	NA	3.47×10^{-13}
3	M	83	Adverse	9.38×10^{10}	7.271	0.721	8.82×10^{-13}
4	M	79	Favorable	2.35×10^{11}	5.355	NA	1.61×10^{-12}
5	M	92	Adverse	1.95×10^{11}	4.839	NA	2.35×10^{-12}
6	M	73	Intermediate	3.65×10^{11}	2.516	NA	2.39×10^{-12}
7	M	83	Adverse	1.64×10^{11}	8.423	NA	3.32×10^{-12}
8	F	89	Adverse	1.45×10^{11}	0.558	0.844	3.86×10^{-12}
9	M	59	Adverse	9.36×10^{10}	2.211	0.852	4.08×10^{-12}
10	M	75	Adverse	5.40×10^{10}	6.161	NA	5.67×10^{-12}
11	M	63	Favorable	7.04×10^{10}	NA	NA	6.65×10^{-12}
12	M	58	Adverse	1.62×10^{11}	NA	NA	NA
13	M	87	Adverse	1.10×10^{11}	2.288	NA	NA
14	M	70	Adverse	1.79×10^{11}	NA	NA	NA
15	M	73	Adverse	1.23×10^{11}	1.334	NA	NA
16	F	71	Intermediate	2.84×10^{11}	NA	0.936	3.14×10^{-12}
17	M	65	Adverse	5.76×10^{10}	NA	0.790	1.27×10^{-11}
18	M	71	Adverse	4.38×10^{11}	NA	0.606	NA

ELN: European Leukemia Net; EVs: extracellular vesicles; F: Female; M: Male; NA: not available.

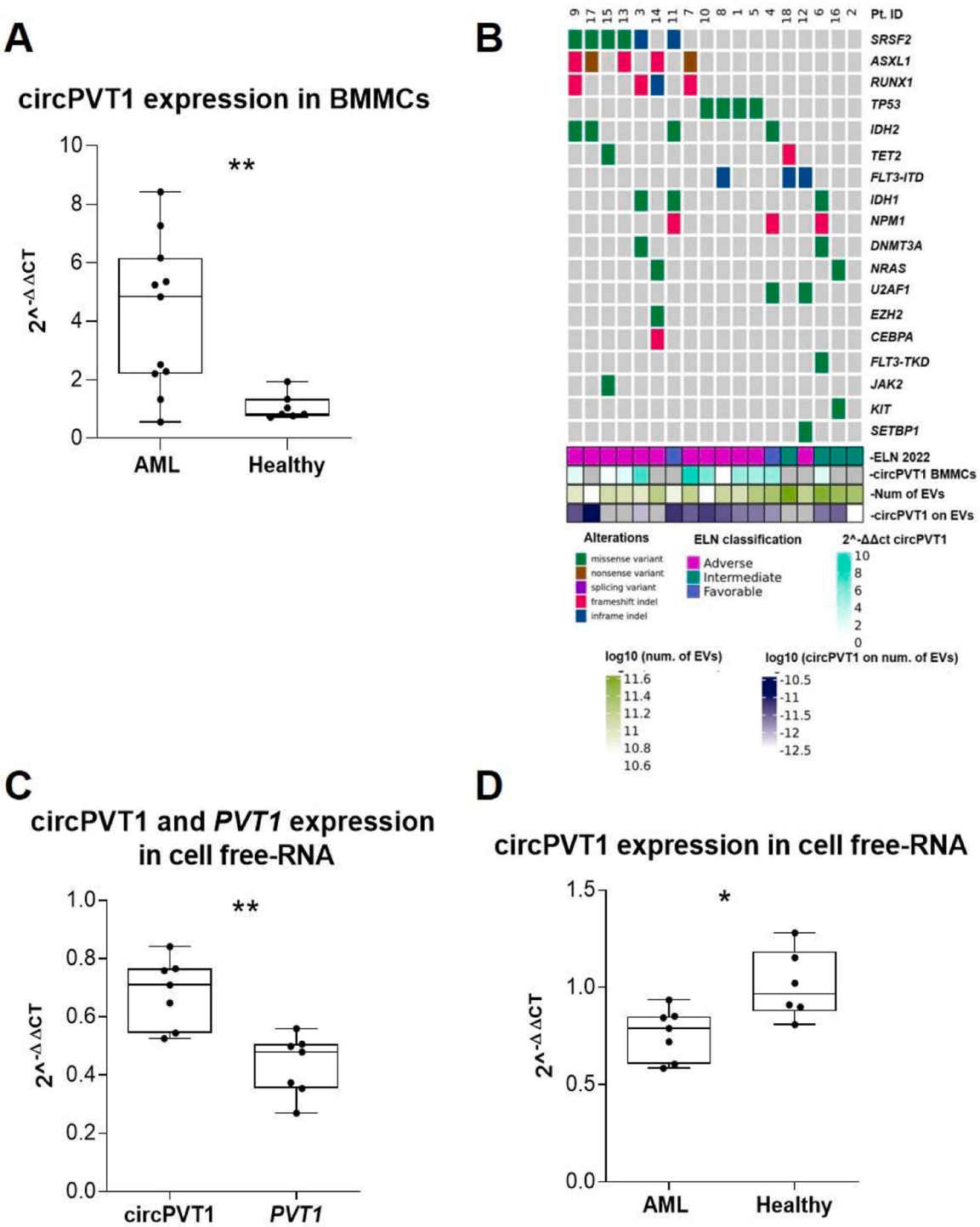

Fig. 1. Intracellular and extracellular levels of circPVT1 in AML patients. A) circPVT1 expression in BMMCs from AML patients (n = 11) and $CD34^+$ cells from healthy subjects (n = 7) by qRT-PCR. B) Mutational status of AML-related genes in our cohort (mutations with a frequency >5% in the analyzed population are reported). Rows denote genes, ELN classification, circPVT1 expression in AML BMMCs, EVs number and circPVT1 expression inside EVs (grey squares in the lower panel indicate missing data). Columns represent patients. C) Cell-free RNA analysis of circPVT1 and linear *PVT1* in the plasma of AML patients (n = 7). D) Cell-free RNA analysis of circPVT1 in the plasma of AML patients (n = 7) and healthy subjects (n = 6; *, $p \leq 0.05$; **, $p \leq 0.01$).

3.3. Analysis of EV surface markers profile in AML

To gain insights into the origin and features of AML microvesicles, we characterized the surface protein profile of isolated circulating EVs by multiplex bead-based flow cytometry assay. Common exosome markers (CD9, CD81 and CD63) were expressed on the surface of microvesicles from both cohorts, with a higher CD9 signals in AML patients EVs (Fig. 3).

Thirteen out of the 37 evaluated markers showed significant differences between AML patients and healthy subjects. Specifically, compared with healthy subjects, EVs from AML patients expressed higher levels of leukemic cells markers (CD133/1, CD105, CD49e) and of CD24 and CD25, which characterize mature granulocytes, B and T cells, respectively, but can be also detected on AML cells [21–24].

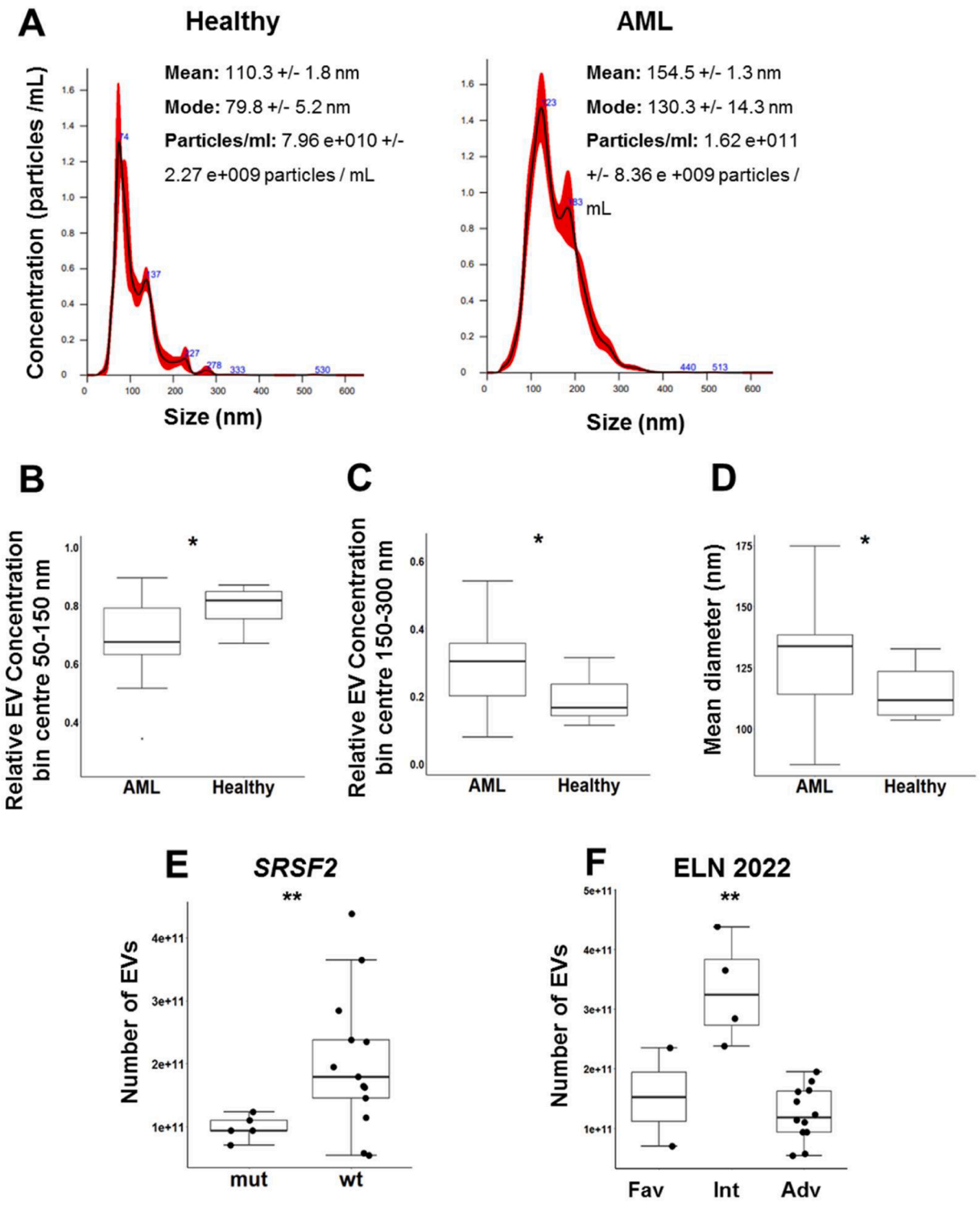

Fig. 2. EVs size and concentration in the plasma of AML patients and healthy subjects. A) Representative NTA profiles of EV-enriched SEC fractions obtained from AML patients and healthy subjects. Relative concentrations of EVs B) with 50–150 nm diameter (50–150 nm EV concentrations/total EV concentrations) or C) with 150–300 nm diameter (150–300 nm EV concentrations/total EV concentrations in AML patients (n = 18) and healthy subjects (n = 12). D) Mean diameter of EVs from AML patients and healthy subjects. E) Boxplot showing the relative EV concentration in the plasma of *SRSF2*-mutated (mut) compared with wildtype (wt) patients. **F)** Boxplot showing the relative EV concentration in the plasma of AML patients according to ELN 2022 classification (Fav: favorable; Int: intermediate; Adv: adverse; *, $p \leq 0.05$; ** $p \leq 0.01$).

Moreover, EVs from AML patients were enriched in B cell (CD20), monocyte/macrophage (CD14) markers, and markers expressed on antigen presenting cells, as dendritic cells and macrophages (CD1c, CD209, CD40, CD86, Fig. 4).

Other markers including CD44, CD29, CD31 and CD4 were expressed with no significant difference between EVs from AML patients and healthy subjects. Conversely, we observed a complete absence of CD3 expression in the EVs from both cohorts. Overall, this data suggest that EVs secreted by myeloid blasts and immune cells likely coexist in the plasma of AML patients. We then analyzed the surface EV markers

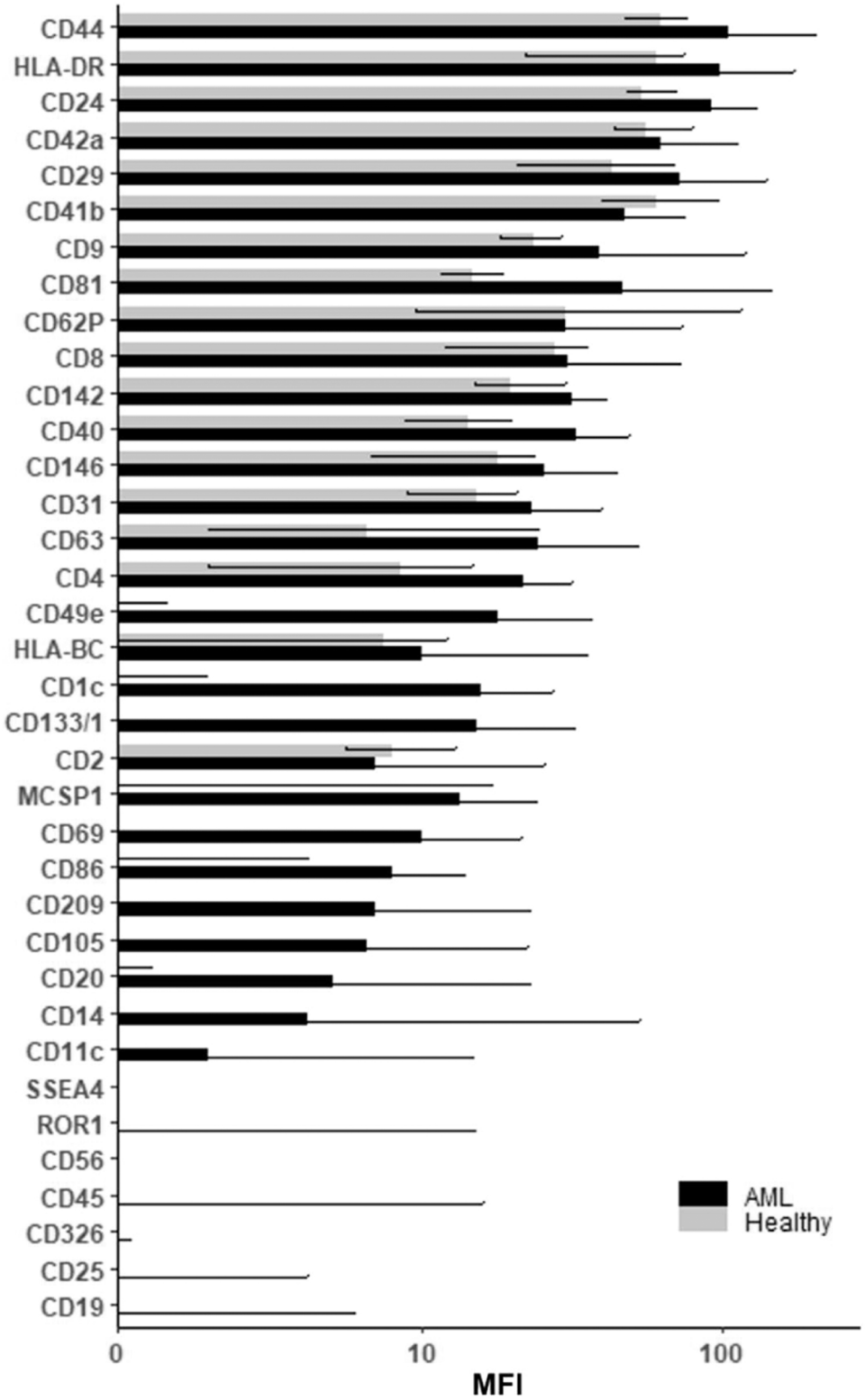

Fig. 3. Surface protein profile of EVs from the plasma of AML patients and healthy subjects. The graphic shows the MFI ± 1–3 quartile (AML, n = 18; healthy, n = 12). Blank control was used for normalization.

showing increased expression in light of the patients' genomic features. Noteworthy, the expression of EV markers differed among AML molecular subgroups, with lower CD86 in *IDH1*-mut ($p = 0.03$, Fig. 5A) and higher CD86 in *TP53*-mut ($p = 0.04$, Fig. 5B) and CD20 in *SRSF2*-mut ($p = 0.01$, Fig. 5C) AML. Moreover, we observed elevated CD45 ($p = 0.03$, Fig. 5D), CD105 ($p = 0.05$, Fig. 5E) and CD133/1 ($p = 0.03$, Fig. 5F) in EVs from *TET2*-mut compared to wild-type cases.

3.4. Detection of circPVT1 cargo inside AML EVs

Since circPVT1 is overexpressed in leukemic compared with normal stem-progenitor cells and it is also present at extracellular level in the

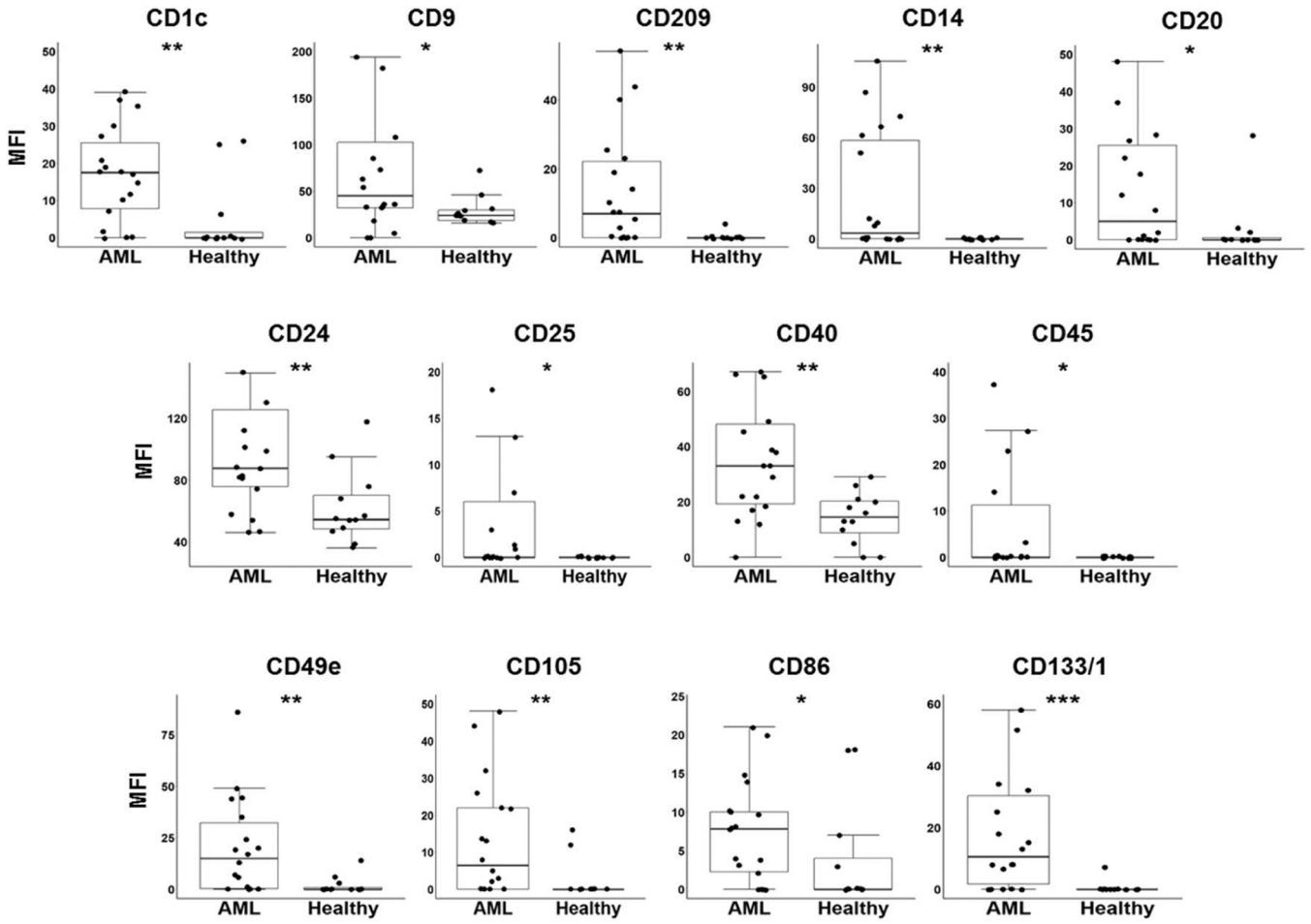

Fig. 4. Differentially expressed surface markers between AML and healthy Evs. Box plots of EV protein expression analysis in AML patients and healthy subjects. (*, $p \leq 0.05$; **, $p \leq 0.01$; ***, $p \leq 0.001$).

patients' plasma, we asked whether EVs from AML patients contain circPVT1. Our digital PCR analysis showed that EVs from AML patients have higher levels of circPVT1 cargo compared with EVs from healthy subjects (Fig. 6). Moreover, no correlation was observed between the circPVT1 levels inside EVs and the percentage of circulating leukemic blasts (Spearman rank correlation: R=−0.32, $p = 0.41$).

4. Discussion

Several studies have described a role of EVs in cell-to-cell and cell-to-environment communication [25]. EVs are crucial for the release of signals driving hematopoietic stem cell differentiation and fate in the healthy immune system [26]. Here we found that EVs isolated from the AML patients are larger compared with those found in the plasma of healthy subjects, which may be linked to an increased molecular cargo. This evidence is in line with the findings from Szczepansk *et al.* that reported a significantly greater protein content in serum EVs from AML patients compared with those isolated from healthy controls [27]. It is not clear whether the size increase is strictly related to EVs secreted by the leukemic blasts or those released by immune cells, activated platelets or the endothelium also contribute to this phenotype. Based on their surface profile, EVs originated from leukemic cells are clearly present in the patients' plasma. Unfortunately, important proteins as CD34, CD33 and CD117, which are typically expressed by AML blasts, are not detected by the commercial panel we used. However, we observed a higher expression of CD133/1 and CD105 stem cell markers in EVs from AML patients compared with healthy subjects [28,29]. In solid tumors, CD133 expression associates with stem cell properties, including self-renewal, proliferation, differentiation into diverse cell types and tumor engraftment in xenograft models [30]. Both CD133 and CD105 are expressed by $CD34^{+}CD38^{-}$ leukemia stem cells (LSCs) [31]. Our results showing high CD133/1 EV expression in cases harbouring *TET2* mutations, which is expected to cause a loss of function, are in line with previous data reporting reduced *TET2* expression in $CD133^{+}$ cells from heptocellular carcinoma patients [32]. Moreover, CD105 and CD34 co-expression characterized a group of long-term repopulating haematopoietic stem cells (HSCs) playing a pivotal role for maintaining the HSC pool. Specifically, CD105 seems to be necessary for re-entry into the quiescence state [33,34]. The CD49e integrin is highly expressed by EVs from AML patients and by leukemic cells themselves. Its altered expression has been suggested to be implicated in the interaction between leukemic and mesenchymal stromal cells, resulting in increased cell adhesion and in promotion of AML cell survival and growth [35]. Accordingly, CD49e expression on EVs could increase the binding of leukemia-derived vesicles to mesenchymal stromal cells, thus facilitating the uptake of their cargo content. The high CD25 expression on AML EVs is also interesting, since this marker distinguishes LSCs from normal bone marrow stem cells [36], while being also a marker of regulatory T cells, that are over-represented in AML patients [37]. Moreover, we reported here a negative association between EV concentration and *SRSF2* mutation, in line with low number of EV in the adverse risk subgroup. We also observed high and low CD86 EV levels in *TP53*-mut and *IDH1*-mut cases, respectively, which may be supported by previous data obtained in malignant cells from AML [38] and gliomas [39]. To our knowledge, this is the first study that correlates EVs and their content with AML molecular profile.

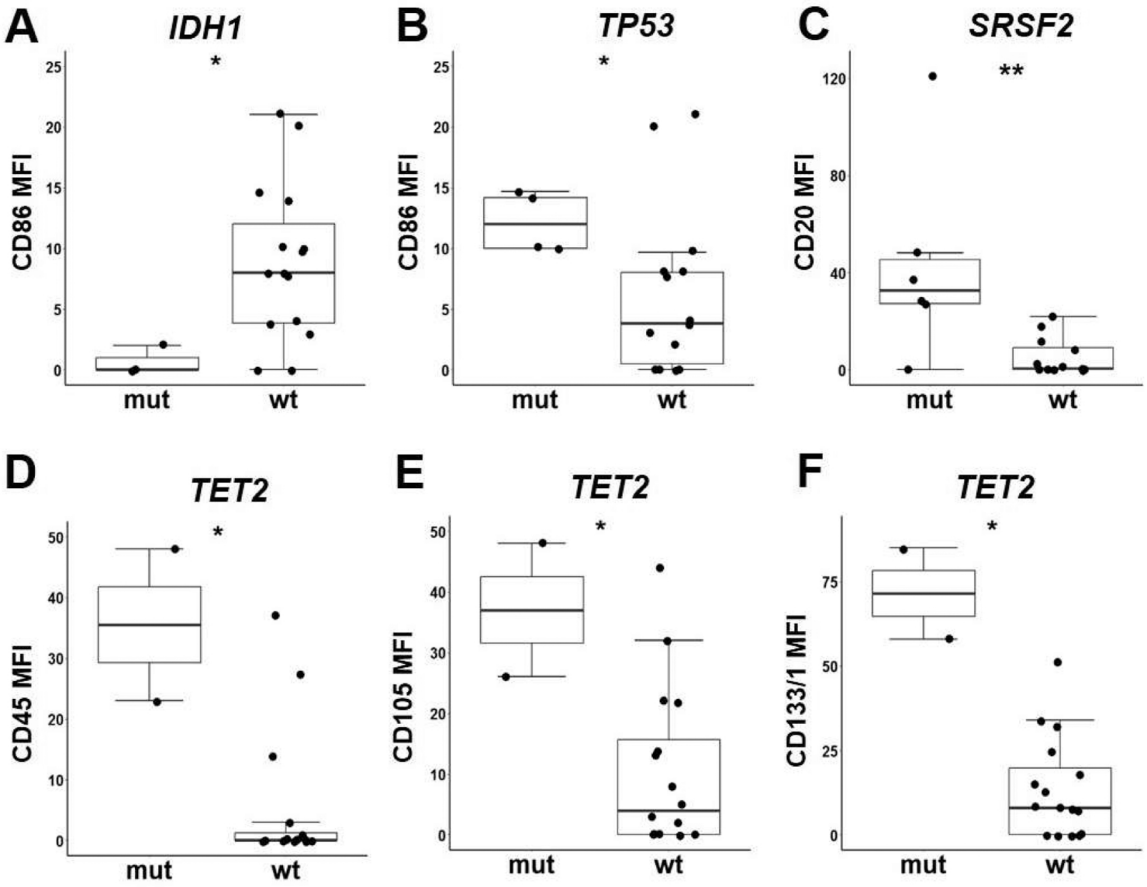

Fig. 5. Differences in the expression of EV markers according to the mutational status of AML-related genes. Box plots showing the MFI of A) CD86 in *IDH1*-mutated (mut) *versus* wild-type (wt) cases, B) CD86 in *TP53*-mut *versus* wt cases), C) CD20 in *SRSF2*-mut *versus* wt cases, D) CD45, E) CD105, F) CD133/1 in *TET2*-mut *versus* wt cases (*, $p \leq 0.05$; **, $p \leq 0.01$).

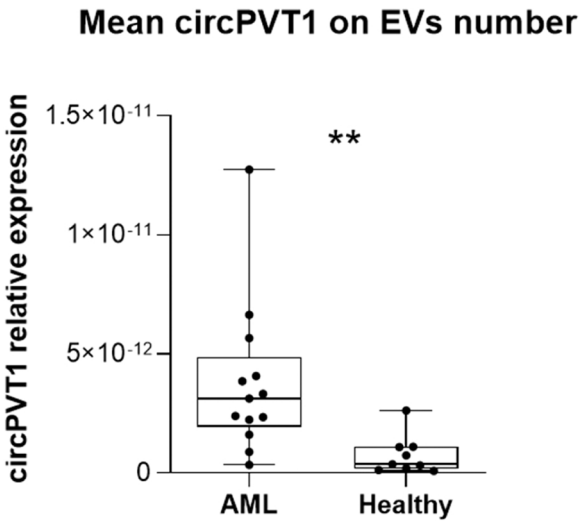

Fig. 6. EV levels of circPVT1. circPVT1 quantification by dPCR inside EVs of AML patients (n = 13) and healthy subjects (n = 8). Data were normalized on EVs number. (**, $p \leq 0.01$).

In AML, EVs released from blast cells can modify the microenvironment through the release of regulatory molecules shaping gene expression and cellular phenotypes [40], in order to evade the antileukemic response and support malignant cell growth [41].

While evidence is available through the literature regarding the immunoregulatory role of *PVT1* and/or circPVT1 under infection, inflammatory conditions and autoimmune disease, little is known about their function in the tumor microenvironment. Recent data indicate that high expression of linear *PVT1* by granulocytic myeloid-derived suppressor cells contributed to the suppression of T cell- induced antitumor immune responses in murine models of Lewis lung carcinoma and colorectal cancer [42].

To understand whether *PVT1* and circPVT1 may function as messengers released by leukemic blasts, we analyzed cell-free RNA from patients' plasma. Both linear and circular isoforms were detectable as cell-free RNA in patients' plasma. However, circPVT1 is more abundant than its linear counterpart, likely due to its properties,including size and secondary structure, that maks it more suitable to be packaged inside EVs. We here showed that the increased circPVT1 expression observed in AML blasts compared to normal $CD34^+$ cells reflects into higher circPVT1 cargo inside EVs from AML patients compared with healthy subjects. Conversely, cell-free circPVT1 levels were lower in patients compared with healthy subjects. These findings are in line with previous miRNA studies, reporting higher miR-101, miR-372 and miR-373 levels in cancer cases compared to healthy controls, when considering miRNA isolated from exosomes, but not overall serum RNA [43]. We can hypothesize that the EV membrane protects the RNA cargo from degradation in the bloodstream, thus providing a more effective reservoir of miRNAs and other RNAs in terms of interplay with the microenvironment [44]. This hypothesis and the molecular associations that we describe throughout the work need to be corroborated in larger patients cohorts, since one limitation of our work resides in the low number of analyzed patients. Moreover, the same results deserve further investigation to address the functional mechanisms behind them.

In conclusion, our work highlights specific features of AML EVs in terms of size, concentration, surface markers and cargo content. In particular, we here show that circPVT1 cargo is enriched in EVs from AML patients compared with healthy subjects, suggesting a potential role in the crosstalk between blast cells and the tumor microenvironment.

Sources of Funding

This work was supported by Associazione Italiana contro le leucemie-linfomi e mieloma (AIL) Treviso.

Disclosure

GM has competing interests with Novartis, BMS, Roche, Pfizer, ARIAD, MSD. The other authors declare that they have no competing interest.

CRediT authorship contribution statement

Martina Ghetti: Conceptualization, Methodology, Investigation, Writing – original draft, Visualization. **Ivan Vannini**: Conceptualization, Methodology, Investigation, Writing – original draft. **Maria Teresa Bochicchio**: Data curation, Writing – review & editing. **Irene Azzali**: Formal analysis, Writing – review & editing. **Lorenzo Ledda**: Methodology. **Giovanni Marconi**: Conceptualization, Resources, Writing – review & editing. **Mattia Melloni**: Methodology. **Francesco Fabbri**: Conceptualization, Writing – review & editing. **Michela Rondoni**: Resources. **Roberta Chicchi**: Resources. **Davide Angeli**: Software, Formal analysis, Writing – review & editing. **Andrea Ghelli Luserna di Rorà**: Methodology, Writing – review & editing. **Barbara Giannini**: Resources. **Irene Zacheo**: Conceptualization, Resources, Writing – review & editing. **Rino Biguzzi**: Resources. **Francesco Lanza**: Resources. **Giovanni Martinelli**: Supervision, Funding acquisition. **Giorgia Simonetti**: Conceptualization, Investigation, Validation, Writing – original draft, Supervision, Project administration.

Declaration of Competing Interest

The other authors declare that they have no competing interest.

Data availability

Data will be made available on request.

Appendix A. Supporting information

Supplementary data associated with this article can be found in the online version at doi:10.1016/j.biopha.2023.115235.

References

[1] D. Duarte, E.D. Hawkins, C. Lo Celso, The interplay of leukemia cells and the bone marrow microenvironment, Blood (2018), https://doi.org/10.1182/blood-2017-12-784132.
[2] B. Kumar, M. Garcia, L. Weng, X. Jung, J.L. Murakami, X. Hu, T. McDonald, A. Lin, A.R. Kumar, D.L. Digiusto, A.S. Stein, V.A. Pullarkat, S.K. Hui, N. Carlesso, Y. H. Kuo, R. Bhatia, G. Marcucci, C.C. Chen, Acute myeloid leukemia transforms the bone marrow niche into a leukemia-permissive microenvironment through exosome secretion, Leukemia (2018), https://doi.org/10.1038/leu.2017.259.
[3] M. Boyiadzis, T.L. Whiteside, The emerging roles of tumor-derived exosomes in hematological malignancies, Leukemia (2017), https://doi.org/10.1038/leu.2017.91.
[4] Y.F. Mustafa, Chemotherapeutic Applications of Folate Prodrugs: A Review, Neuroquantology 19 (2021) 99–112, https://doi.org/10.14704/nq.2021.19.8.NQ21120.
[5] C.S. Hong, P. Sharma, S.S. Yerneni, P. Simms, E.K. Jackson, T.L. Whiteside, M. Boyiadzis, Circulating exosomes carrying an immunosuppressive cargo interfere with cellular immunotherapy in acute myeloid leukemia, Sci. Rep. (2017), https://doi.org/10.1038/s41598-017-14661-w.
[6] C.S. Hong, L. Muller, M. Boyiadzis, T.L. Whiteside, Isolation and characterization of CD34+ blast-derived exosomes in acute myeloid leukemia, PLoS One (2014), https://doi.org/10.1371/journal.pone.0103310.
[7] C.S. Hong, G. Danet-Desnoyers, X. Shan, P. Sharma, T.L. Whiteside, M. Boyiadzis, Human acute myeloid leukemia blast-derived exosomes in patient-derived xenograft mice mediate immune suppression, Exp. Hematol. (2019), https://doi.org/10.1016/j.exphem.2019.07.005.
[8] K.K. Ebbesen, T.B. Hansen, J. Kjems, Insights into circular RNA biology, RNA Biol. 14 (2017) 1035–1045, https://doi.org/10.1080/15476286.2016.1271524.
[9] Y. Liu, Z. Cheng, Y. Pang, L. Cui, T. Qian, L. Quan, H. Zhao, J. Shi, X. Ke, L. Fu, Role of microRNAs, circRNAs and long noncoding RNAs in acute myeloid leukemia, J. Hematol. Oncol. (2019), https://doi.org/10.1186/s13045-019-0734-5.
[10] E. Lasda, R. Parker, Circular RNAs co-precipitate with extracellular vesicles: A possible mechanism for circrna clearance, PLoS One (2016), https://doi.org/10.1371/journal.pone.0148407.
[11] A.H. Amin, L.M. Al Sharifi, A.J. Kakhharov, M.J.C. Opulencia, F. Alsaikhan, D. O. Bokov, H.S. Majdi, M.A. Jawad, A.T. Hammid, M.N. Shalaby, Y.F. Mustafa, H. Siahmansouri, Role of Acute Myeloid Leukemia (AML)-Derived exosomes in tumor progression and survival, Biomed. Pharmacother. (2022), https://doi.org/10.1016/j.biopha.2022.113009.
[12] D. Wang, X. Ming, J. Xu, Y. Xiao, Circ_0009910 shuttled by exosomes regulates proliferation, cell cycle and apoptosis of acute myeloid leukemia cells by regulating miR-5195-3p/GRB10 axis, Hematol. Oncol. (2021), https://doi.org/10.1002/hon.2874.
[13] J. Bi, Y. Pu, X. Yu, Exosomal circ_0004136 enhances the progression of pediatric acute myeloid leukemia depending on the regulation of miR-570-3p/TSPAN3 axis, Anticancer. Drugs (2021), https://doi.org/10.1097/CAD.0000000000001068.
[14] M. Ghetti, I. Vannini, C.T. Storlazzi, G. Martinelli, G. Simonetti, Linear and circular PVT1 in hematological malignancies and immune response: Two faces of the same coin, Mol. Cancer (2020), https://doi.org/10.1186/s12943-020-01187-5.
[15] D. Traversa, G. Simonetti, D. Tolomeo, G. Visci, G. Macchia, M. Ghetti, G. Martinelli, L.S. Kristensen, C.T. Storlazzi, Unravelling similarities and differences in the role of circular and linear PVT1 in cancer and human disease, Br. J. Cancer (2022), https://doi.org/10.1038/s41416-021-01584-7.
[16] T. Chen, F. Chen, The role of circular RNA plasmacytoma variant translocation 1 as a biomarker for prognostication of acute myeloid leukemia, Hematol. (U. Kingd.) (2021), https://doi.org/10.1080/16078454.2021.1987649.
[17] C.X. Liu, X. Li, F. Nan, S. Jiang, X. Gao, S.K. Guo, W. Xue, Y. Cui, K. Dong, H. Ding, B. Qu, Z. Zhou, N. Shen, L. Yang, L.L. Chen, Structure and Degradation of Circular RNAs Regulate PKR Activation in Innate Immunity, e21, Cell 177 (2019) 865–880, https://doi.org/10.1016/j.cell.2019.03.046.
[18] Z. Gu, R. Eils, M. Schlesner, Complex heatmaps reveal patterns and correlations in multidimensional genomic data, Bioinformatics (2016), https://doi.org/10.1093/bioinformatics/btw313.
[19] R. Sanders, D.J. Mason, C.A. Foy, J.F. Huggett, Evaluation of Digital PCR for Absolute RNA Quantification, PLoS One (2013), https://doi.org/10.1371/journal.pone.0075296.
[20] K. Tashiro, Y.-Y. Tseng, B. Konety, A. Bagchi, MP99-18 role of long non-coding RNA PVT1 in regulating MYC in human cancer, J. Urol. (2017), https://doi.org/10.1016/j.juro.2017.02.3104.
[21] T.J. Raife, D.J. Lager, J.D. Kemp, F.R. Dick, Expression of CD24 (BA-1) predicts monocytic lineage in acute myeloid leukemia, Am. J. Clin. Pathol. (1994), https://doi.org/10.1093/ajcp/101.3.296.
[22] G. Valet, R. Repp, H. Link, A. Ehninger, M. Gramatzki, Pretherapeutic Identification of High-Risk Acute Myeloid Leukemia (AML) Patients from Immunophenotypic, Cytogenetic, and Clinical Parameters, Cytom. Part B - Clin. Cytom. (2003), https://doi.org/10.1002/cyto.b.10028.
[23] P. Miltiades, E. Lamprianidou, T.P. Vassilakopoulos, S.G. Papageorgiou, A. G. Galanopoulos, S. Vakalopoulou, V. Garypidou, M. Papaioannou, E. Hadjiharissi, V. Pappa, H.A. Papadaki, E. Spanoudakis, K. Tsatalas, I. Kotsianidis, Expression of CD25 antigen on CD34+ cells is an independent predictor of outcome in late-stage MDS patients treated with azacitidine, Blood Cancer J. (2014), https://doi.org/10.1038/bcj.2014.9.
[24] T. Marchand, S. Pinho, Leukemic stem cells: from leukemic niche biology to treatment opportunities, Front. Immunol. (2021), https://doi.org/10.3389/fimmu.2021.775128.
[25] M. Colombo, G. Raposo, C. Théry, Biogenesis, secretion, and intercellular interactions of exosomes and other extracellular vesicles, Annu. Rev. Cell Dev. Biol. (2014), https://doi.org/10.1146/annurev-cellbio-101512-122326.
[26] J.T. Butler, S. Abdelhamed, P. Kurre, Extracellular vesicles in the hematopoietic microenvironment, Haematologica (2018), https://doi.org/10.3324/haematol.2017.183335.
[27] M.J. Szczepanski, M. Szajnik, A. Welsh, T.L. Whiteside, M. Boyiadzis, Blast-derived microvesicles in sera from patients with acute myeloid leukemia suppress natural killer cell function via membrane-associated transforming growth factor-β1, Haematologica (2011), https://doi.org/10.3324/haematol.2010.039743.
[28] D. Pastore, A. Mestice, T. Perrone, F. Gaudio, M. Delia, F. Albano, A. Russo Rossi, P. Carluiccio, M. Leo, V. Liso, G. Specchia, Subsets of CD34+ and early engraftment kinetics in allogeneic peripheral SCT for AML, Bone Marrow Transpl. (2008), https://doi.org/10.1038/bmt.2008.87.
[29] M. Miljkovic-Licina, N. Arraud, A.D. Zahra, P. Ropraz, T. Matthes, Quantification and phenotypic characterization of extracellular vesicles from patients with acute myeloid and B-cell lymphoblastic leukemia, Cancers (Basel) (2022), https://doi.org/10.3390/cancers14010056.
[30] G.Y. Liou, CD133 as a regulator of cancer metastasis through the cancer stem cells, Int. J. Biochem. Cell Biol. (2019), https://doi.org/10.1016/j.biocel.2018.10.013.

[31] W. Zeijlemaker, T. Grob, R. Meijer, D. Hanekamp, A. Kelder, J.C. Carbaat-Ham, Y. J.M. Oussoren-Brockhoff, A.N. Snel, D. Veldhuizen, W.J. Scholten, J. Maertens, D. A. Breems, T. Pabst, M.G. Manz, V.H.J. van der Velden, J. Slomp, F. Preijers, J. Cloos, A.A. van de Loosdrecht, B. Löwenberg, P.J.M. Valk, M. Jongen-Lavrencic, G.J. Ossenkoppele, G.J. Schuurhuis, CD34+CD38− leukemic stem cell frequency to predict outcome in acute myeloid leukemia, Leukemia (2019), https://doi.org/10.1038/s41375-018-0326-3.

[32] C.L. Chen, J.C. Hernandez, D.B. Uthaya Kumar, T. Machida, S.M. Tahara, A. El-Khoueiry, M. Li, V. Punj, S.K. Swaminathan, A. Kirtane, Y. Chen, J. Panyam, K. Machida, Profiling of circulating tumor cells for screening of selective inhibitors of tumor-initiating stem-like cells, Adv. Sci. (2023), https://doi.org/10.1002/advs.202206812.

[33] J. Kauer, K. Schwartz, C. Tandler, C. Hinterleitner, M. Roerden, G. Jung, H.R. Salih, J.S. Heitmann, M. Märklin, CD105 (Endoglin) as negative prognostic factor in AML, Sci. Rep. (2019), https://doi.org/10.1038/s41598-019-54767-x.

[34] H. Glimm, I.H. Oh, C.J. Eaves, Human hematopoietic stem cells stimulated to proliferate in vitro lose engraftment potential during their S/G2/M transit and do not reenter Go, Blood (2000), https://doi.org/10.1182/blood.v96.13.4185.

[35] F.M. Roversi, N.M. Cury, M.R. Lopes, K.P. Ferro, J.A. Machado-Neto, M.C. Alvarez, G.P. dos Santos, R. Giardini Rosa, A.L. Longhini, A. da, S.S. Duarte, F.V. Pericole, P. Favaro, J.A. Yunes, S.T.O. Saad, Up-regulation of SPINT2/HAI-2 by Azacytidine in bone marrow mesenchymal stromal cells affects leukemic stem cell survival and adhesion, J. Cell. Mol. Med (2019), https://doi.org/10.1111/jcmm.14066.

[36] H. Herrmann, I. Sadovnik, G. Eisenwort, T. Rülicke, K. Blatt, S. Herndlhofer, M. Willmann, G. Stefanzl, S. Baumgartner, G. Greiner, A. Schulenburg, N. Mueller, W. Rabitsch, M. Bilban, G. Hoermann, B. Streubel, D.A. Vallera, W.R. Sperr, P. Valent, Delineation of target expression profiles in CD341/CD382 and CD341/CD381 stem and progenitor cells in AML and CML, Blood Adv. (2020), https://doi.org/10.1182/BLOODADVANCES.2020001742.

[37] M.J. Szczepanski, M. Szajnik, M. Czystowska, M. Mandapathil, L. Strauss, A. Welsh, K.A. Foon, T.L. Whiteside, M. Boyiadzis, Increased frequency and suppression by regulatory T cells in patients with acute myelogenous leukemia, Clin. Cancer Res (2009), https://doi.org/10.1158/1078-0432.CCR-08-3010.

[38] L. yi Zhang, Y. Jin, P. hui Xia, J. Lin, J. chun Ma, T. Li, Z. qi Liu, H. lin Xiang, C. Cheng, Z. jun Xu, H. Zhou, J. Qian, Integrated analysis reveals distinct molecular, clinical, and immunological features of B7-H3 in acute myeloid leukemia, Cancer Med (2021), https://doi.org/10.1002/cam4.4284.

[39] X. Yan, Q. Zhou, H. Zhu, W. Liu, H. Xu, W. Yin, M. Zhao, X. Jiang, C. Ren, The clinical features, prognostic significance, and immune heterogeneity of CD37 in diffuse glioma, IScience 24 (2021), 103249, https://doi.org/10.1016/j.isci.2021.103249.

[40] J. Nehrbas, J.T. Butler, D.W. Chen, P. Kurre, Extracellular vesicles and chemotherapy resistance in the AML microenvironment, Front. Oncol. (2020), https://doi.org/10.3389/fonc.2020.00090.

[41] K.N. Miyamoto, D. Bonatto, Circulating cells and exosomes in acute myelogenous leukemia and their role in disease progression and survival, Clin. Immunol. (2020), https://doi.org/10.1016/j.clim.2020.108489.

[42] Y. Zheng, X. Tian, T. Wang, X. Xia, F. Cao, J. Tian, P. Xu, J. Ma, H. Xu, S. Wang, Long noncoding RNA Pvt1 regulates the immunosuppression activity of granulocytic myeloid-derived suppressor cells in tumor-bearing mice, Mol. Cancer 18 (2019), https://doi.org/10.1186/s12943-019-0978-2.

[43] C. Eichelser, I. Stückrath, V. Müller, K. Milde-Langosch, H. Wikman, K. Pantel, H. Schwarzenbach, Increased serum levels of circulating exosomal microRNA-373 in receptor-negative breast cancer patients, Oncotarget (2014), https://doi.org/10.18632/oncotarget.2520.

[44] E. Endzelinš, A. Berger, V. Melne, C. Bajo-Santos, K. Sobolevska, A. Abols, M. Rodriguez, D. Šantare, A. Rudnickiha, V. Lietuvietis, A. Llorente, A. Line, Detection of circulating miRNAs: Comparative analysis of extracellular vesicle-incorporated miRNAs and cell-free miRNAs in whole plasma of prostate cancer patients, BMC Cancer (2017), https://doi.org/10.1186/s12885-017-3737-z.